



# Sea shell powder as a new adsorbent to remove Basic Green 4 (Malachite Green) from aqueous solutions: Equilibrium, kinetic and thermodynamic studies

Shamik Chowdhury, Papita Saha\*

Biotechnology Department, National Institute of Technology Durgapur, Mahatma Gandhi Avenue, Durgapur, WB 713209, India

## ARTICLE INFO

### Article history:

Received 24 June 2010

Received in revised form 22 August 2010

Accepted 23 August 2010

### Keywords:

Adsorption  
Sea shell powder  
Basic Green 4  
Equilibrium  
Kinetics  
Thermodynamics

## ABSTRACT

In this work the feasibility of employing sea shell powder to remove Basic Green 4 (BG 4), a cationic dye from its aqueous solutions was investigated. Parameters that influence the adsorption process such as particle size, pH, adsorbent dose, initial dye concentration, contact time and temperature were studied in batch experiments. Optimum adsorption of Basic Green 4 took place at pH 8.0. Further, the adsorbent was characterized by Fourier Transform Infrared Spectroscopy (FTIR) and Scanning Electron Microscopy (SEM). FTIR analysis revealed that  $-OH$ ,  $-CO_3$ , and  $-PO_4$  functional groups were mainly responsible for the adsorption process. The experimental equilibrium adsorption data fitted well to the Langmuir isotherm model. The maximum monolayer adsorption capacity was found to be  $42.33 \text{ mg g}^{-1}$  at 303 K. The kinetic data conformed to the pseudo-second-order kinetic model. Intraparticle diffusion was not the sole rate-controlling factor. The activation energy ( $E_a$ ) of dye adsorption was determined at  $15.71 \text{ kJ mol}^{-1}$  according to Arrhenius equation which indicated that the adsorption process of Basic Green 4 onto sea shell powder may be physical adsorption. Thermodynamic parameters such as Gibbs free energy ( $\Delta G^\circ$ ), enthalpy ( $\Delta H^\circ$ ), and entropy ( $\Delta S^\circ$ ) were also calculated and it was found that the adsorption of dye by sea shell powder was a spontaneous process. It was concluded that sea shell powder has potential for application as adsorbent for removal of Basic Green 4 from aqueous solution.

© 2010 Elsevier B.V. All rights reserved.

## 1. Introduction

Dyes are substances that impart color to a material. Mankind has used dyes since the dawn of civilization [1]. Till the late nineteenth century, all dyes available to man came from natural sources, most commonly from flowers, vegetables, insects, and mollusks [2]. Most of these natural dyes were quite unstable, expensive to produce, difficult to obtain, or hard to use which therefore encouraged the development of synthetic dyes. Synthetic dyes are permanent, quick-setting, easy to use, and are ensured by accurate formulas. In addition, they have an added advantage over natural dyes in terms of color range and availability. Today, nearly, 40,000 dyes and pigments are listed which consist of over 7000 different chemical structures [3]. Approximately 10,000 different dyes and pigments are used industrially and over  $7 \times 10^5$  tonnes are produced annually world-wide [4]. Synthetic dyes are widely used in textile, leather tanning, paper, printing, food, cosmetics, paint, pigments, plastics and pharmaceutical industries, which generate huge volume of wastewater every year [5,6]. The discharge of dyes in the environ-

ment is a matter of concern for both toxicological and esthetical reasons.

Basic Green 4 (BG 4) is an N-methylated diaminotriphenylmethane dye most widely used for coloring purpose among all other dyes of its category [7]. It is an extensively used biocide in the aquaculture industry world-wide. It is also used as a food coloring agent, food additive, a medical disinfectant and anthelmintic as well as a dye in silk, wool, jute, leather, cotton, paper and acrylic industries [6–8]. However there are several reports describing its hazardous and carcinogenic effects [9]. It is highly cytotoxic and carcinogenic to mammalian cells and acts as a liver tumor promoter. It decreases food intake, growth and fertility rates; causes damage to liver, spleen, kidney and heart; inflicts lesions on skin, eyes, lungs and bones. Therefore, the removal of BG 4 from effluents is essential to protect the water resources.

Over the past few decades, several physical, chemical and biological methods have been applied for the removal of dyes from wastewater such as: photocatalytic degradation, sonochemical degradation, micellar enhanced ultrafiltration, cation exchange membranes, electrochemical degradation, adsorption/precipitation processes, integrated chemical–biological degradation, integrated iron(III) photoassisted-biological treatment, solar photo-Fenton and biological processes, and Fenton-biological treatment scheme [10]. As all synthetic dyes used in industries

\* Corresponding author. Tel.: +91 9903739855; fax: +91 3432547375.  
E-mail addresses: [chowdhuryshamik@gmail.com](mailto:chowdhuryshamik@gmail.com) (S. Chowdhury),  
[papitasaha@gmail.com](mailto:papitasaha@gmail.com), [papitasaha@yahoo.co.in](mailto:papitasaha@yahoo.co.in) (P. Saha).

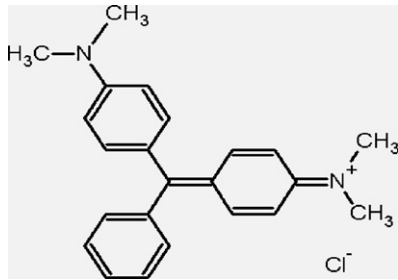
### Nomenclature

$A$	Arrhenius constant
$C_a$	equilibrium dye concentration on the adsorbent ( $\text{mg L}^{-1}$ )
$C_e$	equilibrium dye concentration in solution ( $\text{mg L}^{-1}$ )
$C_i$	initial dye concentration ( $\text{mg L}^{-1}$ )
$E$	mean free energy ( $\text{kJ mol}^{-1}$ )
$E_a$	activation energy ( $\text{kJ mol}^{-1}$ )
$\Delta G^\circ$	Gibbs free energy change ( $\text{kJ mol}^{-1}$ )
$\Delta H^\circ$	enthalpy of reaction ( $\text{kJ mol}^{-1}$ )
$h$	initial adsorption rate ( $\text{mg g}^{-1} \text{min}^{-1}$ )
$I$	intraparticle diffusion model constant
$K_C$	distribution coefficient for adsorption
$K_F$	Freundlich constant ( $\text{mg g}^{-1}$ ) ( $\text{L g}^{-1}$ ) <sup>1/n</sup>
$K_L$	Langmuir constant ( $\text{L mg}^{-1}$ )
$k$	rate constant
$k_i$	intraparticle diffusion rate constant ( $\text{mg g}^{-1} \text{min}^{-0.5}$ )
$k_1$	pseudo-first-order rate constant ( $\text{min}^{-1}$ )
$k_2$	pseudo-second-order rate constant ( $\text{g mg}^{-1} \text{min}^{-1}$ )
$m$	weight of adsorbent (g)
$n$	Freundlich adsorption isotherm constant
$q_e$	equilibrium dye concentration on adsorbent ( $\text{mg g}^{-1}$ )
$q_m$	maximum adsorption capacity ( $\text{mg g}^{-1}$ )
$R$	universal gas constant ( $8.314 \text{ J mol}^{-1} \text{ K}^{-1}$ )
$R^2$	correlation coefficient
$\Delta S^\circ$	entropy of reaction ( $\text{J mol}^{-1} \text{ K}^{-1}$ )
$T$	temperature (K)
$V$	volume of the solution (L)
<i>Greek alphabets</i>	
$\beta$	D–R isotherm constant ( $\text{mmol}^2 \text{ J}^{-2}$ )
$\varepsilon$	Polanyi potential ( $\text{J mmol}^{-1}$ )

are designed to resist fading upon exposure to sweat, light, water, many chemicals including oxidizing agents, and microbial attack, dye-bearing effluents are hardly decolorized by these conventional physico-chemical and biological wastewater treatments methods. This situation has in recent years led to extensive investigations for the development of a method that is highly selective, more efficient, easy to operate and hence cost effective. Adsorption often referred to as passive uptake and physico-chemical binding of chemical species or ions to a solid surface has been suggested as a potential alternative to the existing physical/chemical/biological methods for the removal of dyes from industrial effluents. Adsorption separation in environmental engineering is now an aesthetic attention and consideration abroad the nations, owing to its low initial cost, simplicity of design, ease of operation, insensitivity to toxic substances and complete removal of pollutants even from dilute solutions. A number of investigations have been carried out using natural materials or the wastes/by-products of industries for the removal of dyes from aqueous systems [1]. However, the adsorption capacities of most of the reported adsorbents are still limited [11]. New economical, easily available and highly effective adsorbents are still under development. Hence attempts are made in this study to develop an inexpensive adsorbent for wastewater treatment using sea shell powder.

Sea shell is the hard, protective, outer layer of certain marine animals. In most cases it is the exoskeleton, usually that of an animal without a backbone, an invertebrate. The shell is usually made of outer layers of proteins, followed by an intermediate layer of calcite and a smooth inner layer of platy calcium carbonate

**Table 1**  
Details of the dye used.

Dyestuff	Basic Green 4 (BG 4)
IUPAC name	4-[(4-dimethylaminophenyl)-phenyl-methyl]-N,N-dimethyl-aniline
Commercial name	Malachite Green (MG)
C.I. number	42,000
Appearance	Green crystalline powder
Empirical formula	$\text{C}_{23}\text{H}_{25}\text{N}_2\text{Cl}$
Molecular weight	365
Molecular structure	
$\lambda_{\text{max}}$	621 nm

crystals [12]. Sea shell is an easily available natural material, commonly found in beaches. Shells are very often washed up onto a beach empty and clean, the animal having already died, and the soft parts having rotted away or having been eaten by either predators or scavengers. Every day, thousands of sea shells wash up the shores of the Indian peninsula. Therefore, the availability of sea shell in India is vast. The objective of this study was to investigate and explore the possibility of using sea shell powder for adsorption of BG 4 from aqueous solutions. This study reports for the first time, on the feasibility of applying sea shells as low-cost alternative adsorbent for removal of BG 4 from aqueous solutions. The effects of particle size, adsorbent dose, initial dye concentration, contact time, temperature and pH on dye adsorption using sea shell powder were investigated. Adsorption kinetics, isotherms and thermodynamic parameters were also evaluated and reported.

## 2. Materials and methods

### 2.1. Adsorbent collection and preparation

Bivalve type sea shells that most commonly wash up on large sandy beaches were used in this study. The sea shells were collected from the sea beaches of Puri, Orissa, India. The shells were first thoroughly washed with double distilled water to remove sand, dirt and any unwanted particles. The shells were then dried at  $383 \pm 1 \text{ K}$  for 24 h in an oven drier. The raw adsorbent was then crushed and grounded using ball mill and sieved into the following particle size ranges:  $>500 \mu\text{m}$ ,  $250\text{--}500 \mu\text{m}$  and  $<250 \mu\text{m}$ . Finally, it was stored in sterile, air tight glass bottles and used as adsorbent without any pretreatment for BG 4 adsorption.

### 2.2. Preparation of adsorbate solutions

Basic Green 4 (BG 4) used in this study was of commercial quality and used without further purification. The detailed information of BG 4 used in this study is given in Table 1. Dye stock solution ( $500 \text{ mg L}^{-1}$ ) was prepared by dissolving accurately weighed quantity of the dye in double distilled water. Experimental dye solution of different concentrations was prepared by diluting the stock solution with suitable volume of double distilled water.

### 2.3. Adsorbent characterization

Textural characterization of the prepared sea shell powder was carried out by Quantachrome NOVA 2200C USA, surface area and pore size analyzer. A gas mixture of 22.9 mol% nitrogen and 77.1 mol% helium was used for this purpose. The Brunauer, Emmett, Teller (BET) surface area, pore volume and pore size of the adsorbent were then determined. The existence of the functional groups on the adsorbent surface and their responsibility for dye adsorption are supported by Fourier Transform Infrared (FTIR) analysis. Therefore, FTIR spectra of the adsorbent before and after BG 4 adsorption were taken using FTIR spectrophotometer (Perkin–Elmer Spectrum BX-II Model). The adsorbent was encapsulated in a KBr disk and by pressing the ground material with 8MT pressure bench press, the translucent disks were obtained. The FTIR spectrum was then recorded in the wavenumber range 4000–500  $\text{cm}^{-1}$  at 4  $\text{cm}^{-1}$  spectral resolution. In addition, scanning electron microscopy (SEM) analysis was carried out using a scanning electron microscope (Model Hitachi S-3000N) to study the surface texture and morphology of the adsorbent. Prior to scanning, the adsorbent was coated with a thin layer of gold using a sputter coater to make it conductive.

### 2.4. Batch experiments

The batch tests were carried out in 250 mL glass-stoppered, Erlenmeyer flasks with 100 mL of working volume, with a concentration of 50  $\text{mg L}^{-1}$ . A weighed amount (0.2 g) of adsorbent was added to the solution. The flasks were agitated at a constant speed of 150 rpm for 4 h in an incubator shaker (Model Innova 42, New Brunswick Scientific, Canada) at  $303 \pm 1$  K. The influence of particle size (>500  $\mu\text{m}$ , 250–500  $\mu\text{m}$  and <250  $\mu\text{m}$ ), pH (2.0, 3.0, 4.0, 5.0, 6.0, 7.0, 8.0, 9.0), initial dye concentration (10, 20, 40, 50, 60, 80, 100  $\text{mg L}^{-1}$ ), adsorbent dose (0.5, 1, 2, 3, 4, 5  $\text{g L}^{-1}$ ), contact time (10, 20, 30, 40, 60, 90, 120, 180, and 240 min), and temperature (303, 313, 323, 333 K) were evaluated during the present study. Samples were collected from the flasks at predetermined time intervals for analyzing the residual dye concentration in the solution. The residual amount of dye in each flask was investigated using UV/vis spectrophotometer (Model Hitachi – 2800). The amount of dye adsorbed per unit sea shell powder ( $\text{mg dye per g adsorbent}$ ) was calculated according to a mass balance on the dye concentration using Eq. (1):

$$q_e = \frac{(C_i - C_e)V}{m} \quad (1)$$

where  $C_i$  is the initial dye concentration ( $\text{mg L}^{-1}$ ),  $C_e$  is the equilibrium dye concentration in solution ( $\text{mg L}^{-1}$ ),  $V$  is the volume of the solution (L), and  $m$  is the mass of the adsorbent in g.

The percent removal (%) of dyes was calculated using the following equation:

$$\text{Removal (\%)} = \frac{C_i - C_e}{C_i} \times 100 \quad (2)$$

All adsorption experiments were performed in triplicate, and the mean values were used in data analysis. Control experiments, performed without the addition of adsorbent, confirmed that the sorption of dye on the walls of Erlenmeyer flasks was negligible.

## 3. Theory

### 3.1. Adsorption isotherms

Different isotherm models have been developed for describing sorption equilibrium. Langmuir, Freundlich and Dubinin–Radushkevich (D–R) isotherms were used in the present study.

#### 3.1.1. Langmuir isotherm

The Langmuir sorption isotherm describes that the uptake occurs on a homogeneous surface by monolayer sorption without interaction between adsorbed molecules and is commonly expressed as [13,14]:

$$\frac{C_e}{q_e} = \frac{C_e}{q_m} + \frac{1}{K_L q_m} \quad (3)$$

where  $q_e$  ( $\text{mg g}^{-1}$ ) and  $C_e$  ( $\text{mg L}^{-1}$ ) are the solid phase concentration and the liquid phase concentration of adsorbate at equilibrium respectively,  $q_m$  ( $\text{mg g}^{-1}$ ) is the maximum adsorption capacity, and  $K_L$  ( $\text{L mg}^{-1}$ ) is the adsorption equilibrium constant. The constants  $K_L$  and  $q_m$  can be determined from the slope and intercept of the plot between  $C_e/q_e$  and  $C_e$ .

#### 3.1.2. Freundlich isotherm

The Freundlich isotherm is applicable to non-ideal adsorption on heterogeneous surfaces and the linear form of the isotherm can be represented as [15,16]:

$$\log q_e = \log K_F + \left(\frac{1}{n}\right) \log C_e \quad (4)$$

where  $q_e$  is the equilibrium dye concentration on adsorbent ( $\text{mg g}^{-1}$ ),  $C_e$  is the equilibrium dye concentration in solution ( $\text{mg L}^{-1}$ ),  $K_F$  ( $\text{mg g}^{-1}$ ) ( $\text{L g}^{-1}$ ) $^{1/n}$  is the Freundlich constant related to sorption capacity and  $n$  is the heterogeneity factor.  $K_F$  and  $1/n$  are calculated from the intercept and slope of the straight line of the plot  $\log q_e$  versus  $\log C_e$ .

#### 3.1.3. Dubinin–Radushkevich (D–R) isotherm

The Dubinin–Radushkevich (D–R) isotherm model envisages about the heterogeneity of the surface energies and has the following formulation [17,18]:

$$\ln q_e = \ln q_m - \beta \varepsilon^2 \quad (5)$$

$$\varepsilon = RT \ln \left(1 + \frac{1}{C_e}\right) \quad (6)$$

where  $q_m$  is the maximum adsorption capacity,  $\beta$  is a coefficient related to the mean free energy of adsorption ( $\text{mmol}^2 \text{J}^{-2}$ ),  $\varepsilon$  is the Polanyi potential ( $\text{J mmol}^{-1}$ ),  $R$  is the gas constant ( $8.314 \text{ J mol}^{-1} \text{ K}^{-1}$ ),  $T$  is the temperature (K) and  $C_e$  is the adsorbate equilibrium concentration ( $\text{mg L}^{-1}$ ). The D–R constants  $q_m$  and  $\beta$  can be determined from the intercept and slope of the plot between  $\ln q_e$  and  $\varepsilon^2$ . The constant  $\beta$  gives an idea about the mean free energy  $E$  ( $\text{kJ mol}^{-1}$ ) of adsorption per mole of the adsorbate when it is transferred to the surface of the solid from infinity in the solution and can be calculated using the relationship [19]:

$$E = \frac{1}{\sqrt{2\beta}} \quad (7)$$

If the magnitude of  $E$  is between 8 and 16  $\text{kJ mol}^{-1}$ , the sorption process is supposed to proceed via chemisorption, while for values of  $E < 8 \text{ kJ mol}^{-1}$ , the sorption process is of physical nature [19].

### 3.2. Adsorption kinetics

The pseudo-first-order, pseudo-second-order and intraparticle diffusion kinetic models were used to study the adsorption kinetics of BG 4 and to quantify the extent of uptake in the adsorption process.

### 3.2.1. Pseudo-first-order kinetic model

The linear form of Lagergren's pseudo-first-order equation is given as [20–22]:

$$\log(q_e - q_t) = \log q_e - \frac{k_1}{2.303} t \quad (8)$$

where  $q_t$  and  $q_e$  are the amount of dye adsorbed at time  $t$  and at equilibrium ( $\text{mg g}^{-1}$ ) and  $k_1$  ( $\text{min}^{-1}$ ) is the rate constant of the equation calculated from the slope of the linear plot of  $\log(q_e - q_t)$  versus  $t$ .

### 3.2.2. Pseudo-second-order kinetic model

The pseudo-second-order kinetic model of Ho and McKay [23,24] can be represented in the following form:

$$\frac{t}{q_t} = \frac{1}{k_2 q_e^2} + \frac{1}{q_e} t \quad (9)$$

where  $k_2$  ( $\text{g mg}^{-1} \text{min}^{-1}$ ) is the adsorption rate constant. A plot of  $t/q_t$  versus  $t$  yields a straight line with a slope of  $1/q_e$ . The value of  $k_2$  is determined from the intercept of the plot. The initial adsorption rate  $h$  ( $\text{mg g}^{-1} \text{min}^{-1}$ ) is defined as [25]:

$$h = k_2 q_e^2 \quad (10)$$

### 3.2.3. Intraparticle diffusion model

The intraparticle diffusion equation is given as follows [26,27]:

$$q_t = k_i t^{0.5} + I \quad (11)$$

where  $k_i$  is the intraparticle diffusion rate constant ( $\text{mg g}^{-1} \text{min}^{-0.5}$ ) and  $I$  ( $\text{mg g}^{-1}$ ) is a constant that gives the information regarding the thickness of the boundary layer. According to this model, if the plot of  $q_t$  versus  $t^{0.5}$  gives a straight line, then the adsorption process is controlled by intraparticle diffusion, while, if the data exhibit multi-linear plots, then two or more steps influence the adsorption process [28–30].

### 3.3. Activation energy and thermodynamic parameters

The activation energy  $E_a$  for BG 4 adsorption onto sea shell powder was calculated by the Arrhenius equation:

$$\ln k = \ln A - \frac{E_a}{RT} \quad (12)$$

where  $k$  is the rate constant,  $A$  is the Arrhenius constant,  $E_a$  is the activation energy ( $\text{kJ mol}^{-1}$ ),  $R$  is the gas constant ( $8.314 \text{ J mol}^{-1} \text{ K}^{-1}$ ) and  $T$  is the temperature (K).  $E_a$  can be determined from the slope of a plot of  $\ln k$  versus  $1/T$ .

Thermodynamic behavior of adsorption of BG 4 on sea shell powder was evaluated by the thermodynamic parameters – Gibbs free energy change ( $\Delta G^\circ$ ), enthalpy ( $\Delta H^\circ$ ) and entropy ( $\Delta S^\circ$ ). These parameters were calculated using the following equations:

$$\Delta G^\circ = -RT \ln K_C \quad (13)$$

$$K_C = \frac{C_a}{C_e} \quad (14)$$

$$\Delta G^\circ = \Delta H^\circ - T\Delta S^\circ \quad (15)$$

where  $K_C$  is the distribution coefficient for adsorption,  $C_a$  is the equilibrium dye concentration on the adsorbent ( $\text{mg L}^{-1}$ ) and  $C_e$  is the equilibrium dye concentration in solution ( $\text{mg L}^{-1}$ ). A plot of  $\Delta G^\circ$  versus temperature,  $T$  will be linear with the slope and intercept giving the values of  $\Delta H^\circ$  and  $\Delta S^\circ$ .

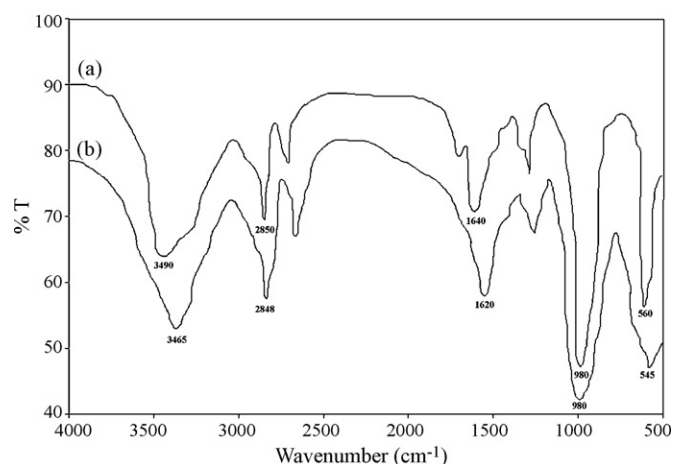


Fig. 1. FTIR spectra of sea shell powder (a) before BG 4 adsorption and (b) after BG 4 adsorption.

## 4. Results and discussion

### 4.1. Adsorbent characterization

The FTIR spectral analysis is important to identify the characteristic functional groups on the surface of the adsorbent, which are responsible for adsorption of dye molecules [31,32]. The FTIR spectrum of sea shell powder was recorded to obtain the information regarding the stretching and bending vibrations of the functional groups which are involved in the adsorption of the adsorbate molecules. The FTIR spectra of sea shell powder before adsorption of BG 4 and that of sea shell powder after BG 4 adsorption is shown in Fig. 1. The FTIR spectral analysis of sea shell powder shows distinct peaks at 3490, 2850, 1640, 980 and 560  $\text{cm}^{-1}$ . The broad and strong band at 3490  $\text{cm}^{-1}$  indicates the presence of –OH stretching. The –CH<sub>2</sub> stretching vibration could be ascribed to the band that appeared at 2850  $\text{cm}^{-1}$ . The strong peak at 1640  $\text{cm}^{-1}$  shows the presence of carbonate group. Absorbance at 980  $\text{cm}^{-1}$  is due to C–O stretching vibration. The characteristic band at 560  $\text{cm}^{-1}$  corresponds to O–P–O bending vibration of phosphate group. Hence FTIR spectral analysis demonstrates the existence of negatively charged functional groups like –CH<sub>2</sub>, –OH, –CO<sub>3</sub>, and –PO<sub>4</sub> on the surface of sea shell powder. After BG 4 adsorption the intensity of hydroxyl, carbonate and phosphate bands of the adsorbent are much greater than those of the adsorbent before adsorption of BG 4. Strong absorption band at 3490  $\text{cm}^{-1}$  (indicative of –OH stretching vibrations) shifted to 3465  $\text{cm}^{-1}$  after BG 4 uptake. The band shift is also observed for –CO<sub>3</sub> and –PO<sub>4</sub> groups moving from 1640 to 1620  $\text{cm}^{-1}$  and 560 to 545  $\text{cm}^{-1}$  respectively. The results suggest that BG 4 interacts with –OH, –CO<sub>3</sub>, and –PO<sub>4</sub> functional group present in sea shell powder.

SEM analysis is another useful tool for the analysis of the surface morphology of an adsorbent. The porous and irregular surface structure of the adsorbent can be clearly observed in the SEM images shown in Fig. 2a. Further, the pores on the surface of the adsorbent are highly heterogeneous as shown in Fig. 2b. The heterogeneous pores and cavities provided a large exposed surface area for the adsorption of BG 4. The sizes of pores are indicative of the expected adsorption of the dye molecules onto the surface of the adsorbent. The BET surface area, total pore volume and average pore diameter of the adsorbent were 3.6  $\text{m}^2 \text{g}^{-1}$ , 0.0065  $\text{cm}^3 \text{g}^{-1}$  and 38 Å, respectively.

### 4.2. Effect of particle size

In the first stage of batch adsorption experiments, the effect of particle sizes on BG 4 adsorption by sea shell powder was investi-

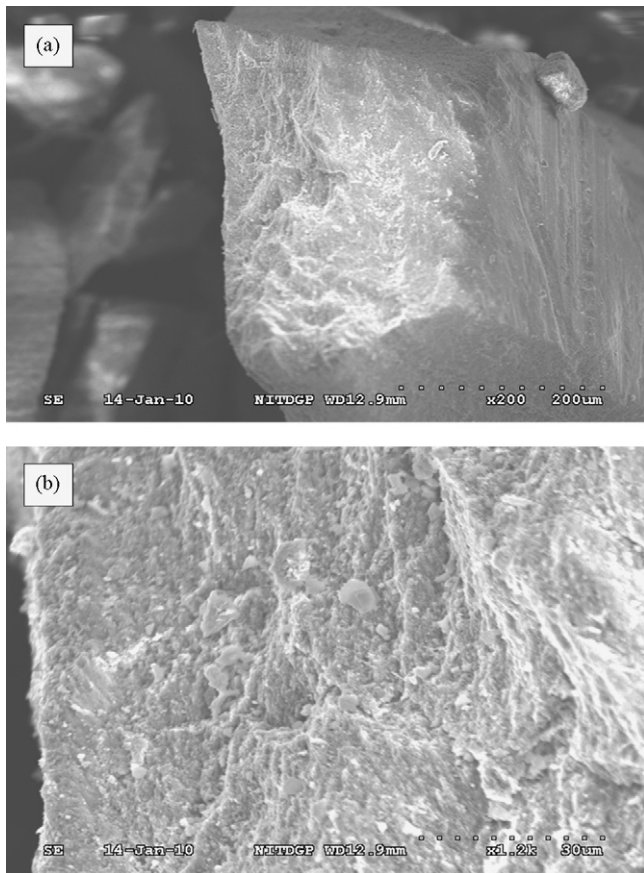


Fig. 2. SEM micrographs of sea shell powder surface (a) magnification 200 $\times$  and (b) magnification 1200 $\times$

gated. Fig. 3 shows the influence of particle size on the adsorption of BG 4 onto sea shell powder. The results illustrated in Fig. 3 shows significant variation in dye uptake capacity at different particle sizes. The amount of dye adsorbed at equilibrium increased by decreasing particle size. For larger particles, the diffusion limitations are usually more significant and consequently the amount of

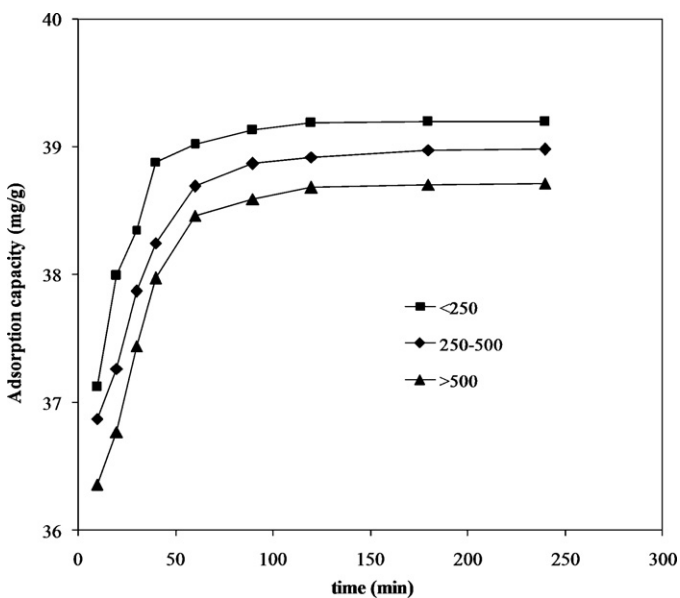


Fig. 3. Effect of particle size on adsorption of BG 4 by sea shell powder (experimental conditions: adsorbent dose: 0.2 g/0.1 L, agitation speed: 150 rpm, temperature: 303 K, contact time: 4 h)

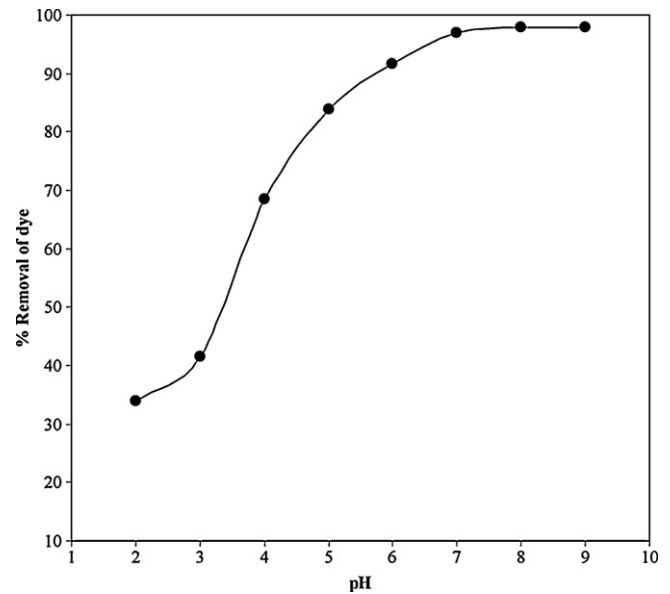
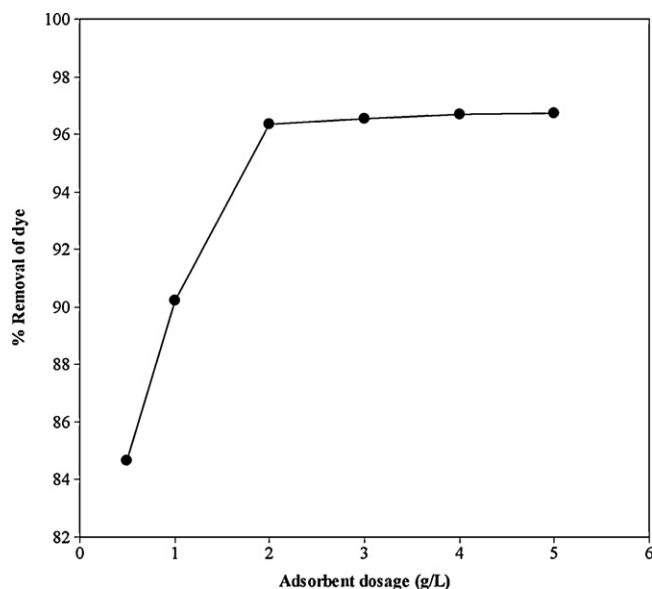


Fig. 4. Effect of pH on adsorption of BG 4 by sea shell powder (experimental conditions: initial dye concentration: 50 mg L<sup>-1</sup>, adsorbent dose: 0.2 g/0.1 L, agitation speed: 150 rpm, temperature: 303 K, contact time: 4 h)

molecules that reach the internal surface of the adsorbent is small resulting in low dye uptake capacity [30]. The breaking down of the large particles to form smaller ones probably serves to open the sealed channels in the adsorbent, which then becomes available for adsorption. The surface area and the number of active pores of the adsorbent increases with the decrease in particle size and therefore result in high dye uptake capacity and removal efficiency [33,34]. Similar observations have been published by Crini et al. [7]. For further experiments, a size fraction of <250  $\mu\text{m}$  was selected because of its high removal capacities.

#### 4.3. Effect of pH

pH has been recognized as one of the most important parameters that affects any adsorption process. It influences the adsorption process by affecting the surface charge of adsorbent, the degree of ionization and speciation of the adsorbate [27]. It is directly related with competition ability of hydrogen ions with adsorbate ions to active sites on the adsorbent surface [14]. Thus the effect of pH on the removal efficiency of BG 4 was studied at different pH ranging from 2.0 to 9.0. Results are shown in Fig. 4. It was observed that a sharp increase in the dye removal occurred when the pH value of the solutions changed from 3.0 to 7.0 and after 7.0 a plateau is obtained. The maximum adsorption of BG 4 occurred in the pH range 7.0–9.0. So, pH 8.0 was selected as optimum pH for BG 4 adsorption onto sea shell powder. The FTIR spectral analysis indicates the involvement of  $-\text{OH}$ ,  $-\text{CO}_3$ , and  $-\text{PO}_4$  functional groups in the adsorption process of BG 4 onto sea shell powder. These groups are protonated at pH values lower than 3.0, and thereby restrict the approach of positively charged dye cations to the surface of the adsorbent. In the pH range of 3.0–9.0, these groups are negatively charged and the adsorption process of BG 4 then proceeds because of electrostatic attraction between the negatively charged adsorbent surface and the positively charged dye cations. The increase in dye removal capacity at higher pH may also be attributed to the reduction of  $\text{H}^+$  ions which compete with dye cations at lower pH for appropriate sites on the adsorbent surface. However with increasing pH, this competition weakens and dye cations replace  $\text{H}^+$  ions bound to the adsorbent surface resulting in increased dye uptake.



**Fig. 5.** Effect of adsorbent dose on adsorption of BG 4 by sea shell powder (experimental conditions: initial dye concentration:  $50 \text{ mg L}^{-1}$ , agitation speed: 150 rpm, pH: 8.0, temperature: 303 K, contact time: 4 h)

#### 4.4. Effect of adsorbent dose

Fig. 5 shows the adsorption profile of BG 4 versus different sea shell powder concentration in the range of  $0.5\text{--}5.0 \text{ g L}^{-1}$ . It was observed that percentage of dye removal increased with increase of adsorbent dose. Such a trend is mostly attributed to an increase in the sorptive surface area and the availability of more active adsorption sites [35]. Although the percentage removal of dye increased with increase of adsorbent dose, the equilibrium adsorption capacity for BG 4 decreased with the increasing amount of adsorbent. This may be due to the decrease in total adsorption surface area available to dye molecules resulting from overlapping or aggregation of adsorption sites [7,36]. Thus with increasing adsorbent mass, the amount of dye adsorbed onto unit mass of adsorbent gets reduced, thus causing a decrease in  $q_e$  value with increasing adsorbent mass concentration. Further, maximum dye removal (96.25%) was observed at  $2.0 \text{ g L}^{-1}$  and further increase in adsorbent dose did not significantly change the adsorption yield. This is due to the binding of almost all dye molecules to adsorbent surface and the establishment of equilibrium between the dye molecules on the adsorbent and in the solution [36]. Quite similar tendency has been reported by Garg et al. for the adsorption of BG 4 by sawdust [37]. The optimum adsorbent dose was found to be  $2.0 \text{ g L}^{-1}$  and was used for the successive experiments.

#### 4.5. Effect of initial dye concentration and contact time

The rate of adsorption is a function of the initial concentration of the adsorbate, which makes it an important factor to be considered for effective adsorption. The effect of different initial BG 4 concentration on adsorption of BG 4 onto sea shell powder is presented in Fig. 6. The percentage removal of dye decreased with increase in initial dye concentration and showed little decrease at higher concentrations. This can be explained that all adsorbents have a limited number of active sites, which become saturated at a certain concentration [38]. However, the adsorption capacity at equilibrium increased with increase in initial dye concentration (not shown in figure). This is due to increasing concentration gradient, acts as increasing driving force to overcome all mass transfer resistances of the BG 4 between the aqueous and solid phase, lead-

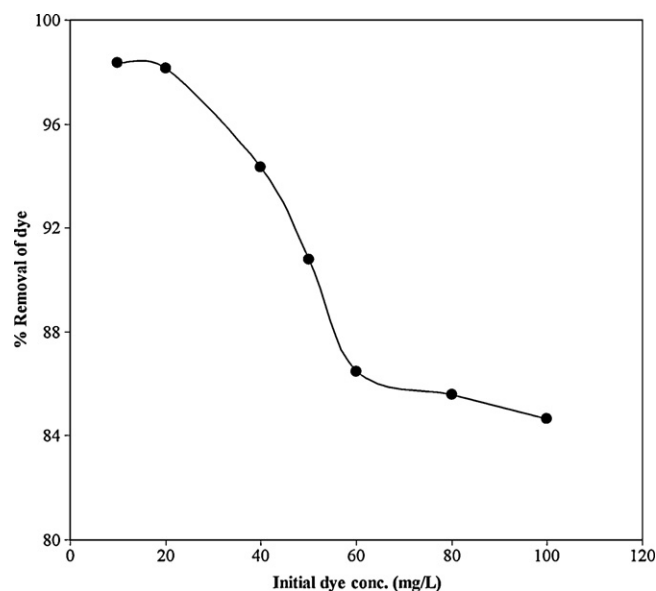


**Fig. 6.** Effect of initial dye concentration on adsorption of BG 4 by sea shell powder (experimental conditions: adsorbent dose:  $0.2 \text{ g}/0.1 \text{ L}$ , agitation speed: 150 rpm, pH: 8.0, temperature: 303 K, contact time: 4 h)

ing to an increasing equilibrium sorption until sorbent saturation is achieved [39]. A similar trend was observed for the adsorption of BG 4 by neem sawdust [40].

The effect of contact time on adsorption of BG 4 was also investigated. It was seen that adsorption of BG 4 increased with rise in contact time up to 90 min (figure not shown). Further increase in contact time did not enhance the adsorption. The adsorption process attained equilibrium after 120 min. The fast adsorption rate at the initial stage may be explained by an increased availability in the number of active binding sites on the adsorbent surface. The sorption rapidly occurs and normally controlled by the diffusion process from the bulk to the surface. In the later stage, the sorption is likely an attachment-controlled process due to less available sorption sites. Similar results have been reported in literature for adsorption of dyes [41–44].

#### 4.6. Effect of temperature

Temperature is a highly significant parameter governing the adsorption process. Increasing temperature modifies the equilibrium capacity of the adsorbent for a particular adsorbate. Therefore, the effect of temperature on BG 4 adsorption by sea shell powder was investigated. Fig. 7 displays the effect of temperature on the adsorption of BG 4 using sea shell powder. As seen from the figure, the percent removal of dye decreased with increasing temperature. The decrease in dye removal with increase in temperature could be due to weakening of the physical bonds between the dye molecules and the active site of the adsorbent. Also with the increase of temperature, the solubility of BG 4 increased. Consequently, the interaction forces between the solute and solvent were stronger than those between solute and adsorbent. As a result, the solute was more difficult to adsorb [45]. The observed trend in decreased dye removal capacity with increasing temperature suggests that the adsorption of BG 4 by sea shell powder is kinetically controlled by an exothermic process.

#### 4.7. Adsorption isotherms

In this investigation, the Freundlich, the Langmuir, and the Dubinin–Radushkevich (D–R) models were used to describe the

**Table 2**  
Adsorption isotherm constants for adsorption of BG 4 onto sea shell powder at different temperatures.

T (K)	Langmuir isotherm parameters			Freundlich isotherm parameters			D–R isotherm parameters			
	$q_m$ (mg g <sup>-1</sup> )	$K_L$ (L mg <sup>-1</sup> )	$R^2$	$K_F$ (mg g <sup>-1</sup> )(L mg <sup>-1</sup> ) <sup>1/n</sup>	1/n	$R^2$	$q_m$ (mg g <sup>-1</sup> )	$\beta$ (mmol <sup>2</sup> J <sup>-2</sup> )	$E$ (kJ mol <sup>-1</sup> )	$R^2$
303	42.331	0.0372	1.0000	7.131	2.898	0.9725	35.106	$1.24 \times 10^{-8}$	6.349	0.9254
313	39.564	0.0311	0.9991	6.748	2.604	0.9512	30.911	$1.30 \times 10^{-8}$	6.197	0.9329
323	37.236	0.0266	0.9999	6.115	2.207	0.9689	29.337	$1.47 \times 10^{-8}$	5.825	0.9082
333	35.619	0.0194	0.9996	5.617	2.044	0.9774	25.892	$1.41 \times 10^{-8}$	5.957	0.9269

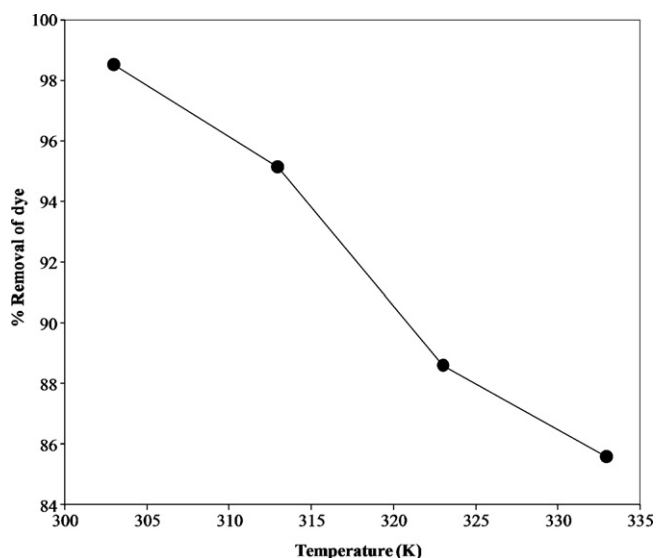


**Fig. 7.** Effect of temperature on adsorption of BG 4 by sea shell powder (experimental conditions: initial dye concentration: 50 mg L<sup>-1</sup>, adsorbent dose: 0.2 g/0.1 L, agitation speed: 150 rpm, pH: 8.0, contact time: 4 h)

equilibrium data acquired at different temperatures. The results are shown in Table 2 and the modelled isotherms are plotted in Fig. 8.

The Langmuir isotherm constants  $K_L$  and  $q_m$  were calculated from the slope and intercept of the plot between  $C_e/q_e$  and  $C_e$  the isotherm showed good fit to the experimental data with high corre-

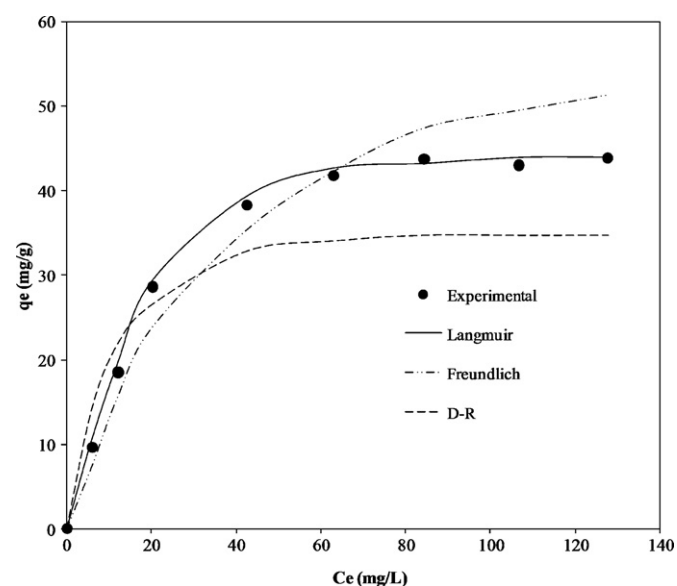


**Fig. 8.** Comparison between the measured and modelled isotherm profiles for the adsorption of BG 4 by sea shell powder (experimental conditions: initial dye concentration: 50 mg L<sup>-1</sup>, adsorbent dose: 0.2 g/0.1 L, agitation speed: 150 rpm, pH: 8.0, temperature: 303 K)

lation coefficients at all temperatures (Table 2). The maximum dye sorption capacity of sea shell powder was found to be 42.33 mg g<sup>-1</sup> at 303 K and pH 8.0. The values of  $K_L$  decreased with the increase in temperature, indicating that increasing temperature induced a lower maximum adsorption capacity.

The Freundlich constants  $K_F$  and  $1/n$  were calculated from the intercept and slope of the straight line of the plot  $\log q_e$  versus  $\log C_e$ . From Table 2, it is seen that the sorption capacity ( $K_F$ ) decreased with increase in temperature. The magnitude of  $n$  gives a measure of favorability of adsorption. The values of  $n$  between 1 and 10 (i.e.,  $1/n$  less than 1) represents a favorable sorption. For the present study the value of  $n$  also presented the same trend representing a beneficial sorption.

In order to distinguish between physical and chemical biosorption on the heterogeneous surfaces the equilibrium data were tested with the D–R isotherm model. The plots between  $\ln q_e$  and  $\varepsilon^2$  gave straight lines at all temperatures; the values of constants  $q_m$  and  $\beta$  thus obtained are given in Table 2. The estimated values of  $E$  for the present study were found in the range expected for physical adsorption (Table 2). Thus the sorption of BG 4 on the surface of sea shell powder was physical in nature.

In comparing the linear correlation coefficients of the three isotherms listed in Table 2, it could be concluded that the adsorption of BG 4 onto sea shell powder, best fitted to the Langmuir isotherm equation under the temperature range studied. The fitness of the adsorption data to the Langmuir isotherm implied that the binding energy on the whole surface of the adsorbent was uniform. It also indicated that the adsorbed dye molecules did not interact or compete with each other and that they were adsorbed by forming a monolayer.

#### 4.8. Adsorption kinetics

As mentioned before, three kinetic models i.e., pseudo-first-order, pseudo-second-order and intraparticle diffusion model were applied to investigate the reaction pathways and potential rate limiting steps of the adsorption of BG 4 onto sea shell powder.

The pseudo-first-order equation did not provide an accurate fit to the experimental data. The first-order rate constant,  $k_1$ , the correlation coefficient,  $R^2$  and theoretical and experimental equilibrium adsorption capacity  $q_e$  are given in Table 3. The  $\log(q_e - q_t)$  versus  $t$  plot (not shown) were linear with  $R^2$  varying from 0.942 to 0.968. However, the theoretical and experimental equilibrium adsorption capacities,  $q_e$  obtained from these plots varied widely, suggesting that the pseudo-first-order model was not appropriate for describing the adsorption kinetics of BG 4 onto sea shell powder.

Further the kinetic data was fitted to the pseudo-second-order equation. The plot of  $t/q_t$  against  $t$  at different temperatures is shown in Fig. 9. Contrary to the pseudo-first-order equation, the fitting of the kinetic data in the pseudo-second-order equation showed excellent linearity with high correlation coefficient ( $R^2 > 0.99$ ) over the temperature range of 303–333 K. The data obtained for the pseudo-second-order kinetic model at the four different temperatures is tabulated in Table 3. The initial adsorption rate,  $h$ , as well as the rate constant,  $k_2$  decreased with increase in temperature. The calculated  $q_e$  values were found to be quite

**Table 3**  
Kinetic parameters for adsorption of BG 4 onto sea shell powder.

T (K)	$q_{exp}$ (mg g <sup>-1</sup> )	Pseudo-first-order kinetic model			Pseudo-second-order kinetic model			
		$q_{cal}$ (mg g <sup>-1</sup> )	$k_1$ (min <sup>-1</sup> )	$R^2$	$q_{cal}$ (mg g <sup>-1</sup> )	$k_2$ (g mg <sup>-1</sup> min <sup>-1</sup> )	$h$ (mg g <sup>-1</sup> min <sup>-1</sup> )	$R$
303	40.347	34.787	0.05962	0.9421	41.285	0.00382	65.110	0.9999
313	38.012	22.351	0.05144	0.9685	38.629	0.00319	47.601	0.9997
323	35.346	19.029	0.04721	0.9572	36.021	0.00247	32.048	0.9995
333	32.254	17.353	0.04298	0.9497	32.945	0.00214	23.226	0.9998

**Table 4**  
Activation energy and thermodynamic parameters for adsorption of BG 4 onto sea shell powder.

$E_a$ (kJ mol <sup>-1</sup> )	$(\Delta G^\circ)$ (kJ mol <sup>-1</sup> )				$(\Delta H^\circ)$ (kJ mol <sup>-1</sup> )	$(\Delta S^\circ)$ (J mol <sup>-1</sup> K <sup>-1</sup> )
	303 K	313 K	323 K	333 K		
15.71	-10.34	-8.68	-7.29	-5.85	-53.80	-148.60

close to the experimental  $q_e$  values at all the temperatures studied (303–333 K). So, it was inferred that the adsorption of BG 4 on sea shell powder followed pseudo-second-order kinetics. Similar phenomena have been observed in sorption of BG 4 onto tamarind fruit shell [8].

The effect of intraparticle diffusion resistance on adsorption was evaluated by intraparticle diffusion model to identify the adsorption mechanism. The Weber Morris plots for adsorption of BG 4 on sea shell powder at different temperatures were multi-modal with three distinct regions (figure not shown). The initial curved region corresponds to the external surface uptake, the second stage relates the gradual uptake reflecting intraparticle diffusion as the rate limiting step and final plateau region indicates equilibrium uptake. Based on these results it might be concluded that intraparticle diffusion was involved in BG 4 adsorption onto sea shell powder, but it was not the sole rate determining step. Similar result was previously reported for sorption of BG 4 onto *Arundo donax* root [46].

#### 4.9. Activation energy and thermodynamic parameters

From the pseudo-second-order rate constant  $k_2$  (Table 3), the activation energy  $E_a$  for the adsorption of BG 4 on sea shell powder was determined using the Arrhenius equation (Eq. (12)). By

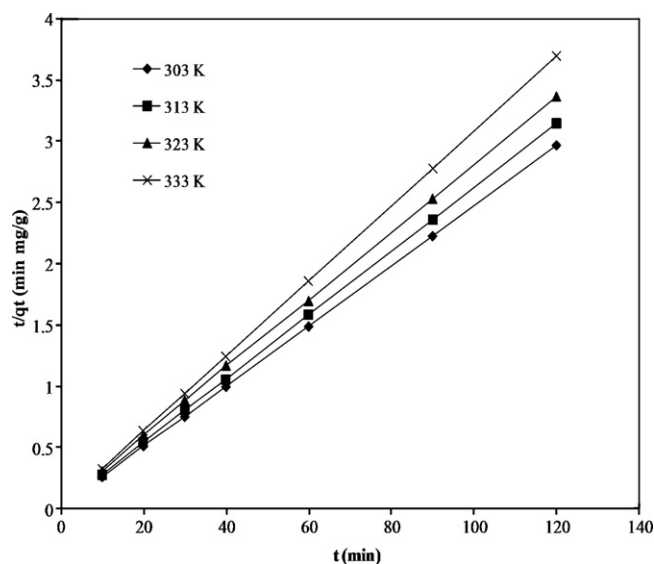


**Fig. 9.** Pseudo-second-order kinetic plots for adsorption of BG 4 onto sea shell powder at different temperatures (experimental conditions: initial dye concentration: 50 mg L<sup>-1</sup>, adsorbent dose: 0.2 g/0.1 L, agitation speed: 150 rpm, pH: 8).

plotting  $\ln k_2$  versus  $1/T$ ,  $E_a$  was obtained from the slope of the linear plot (figure not shown). The value of  $E_a$  for BG 4 adsorption on sea shell powder was 15.71 kJ mol<sup>-1</sup>. The magnitude of activation energy may give an idea about the type of sorption. According to literature, the adsorption process of BG 4 onto sea shell powder may be physical adsorption [47]. The result corresponded well with those from the Dubinin–Radushkevich isotherm

The Gibb's free energy ( $\Delta G^\circ$ ) for the adsorption of BG 4 onto sea shell powder at all temperatures was obtained from Eq. (13) and are listed in Table 4. The values of  $\Delta H^\circ$  and  $\Delta S^\circ$  were determined from the slope and intercept of the plot of  $\Delta G^\circ$  versus  $T$  (figure not shown) and are also listed in Table 4. The negative value of  $\Delta G^\circ$  at all temperatures indicates the feasibility of the process and the spontaneous nature of the dye adsorption on sea shell powder. Increase in value of  $\Delta G^\circ$  with increase in temperature suggests that lower temperature makes the adsorption easier. The negative value of  $\Delta H^\circ$  implies that the adsorption phenomenon is exothermic. The negative value of  $\Delta S^\circ$  suggests the process is enthalpy driven.

#### 4.10. Comparison of sea shell powder with other sorbents

Table 5 summarizes the comparison of the maximum BG 4 adsorption capacities of various sorbents including sea shell powder. The comparison shows that sea shell powder has higher adsorption capacity of BG 4 than many of the other reported adsorbents. The easy availability and cost effectiveness of sea shell

**Table 5**  
Comparison of BG 4 adsorption capacity of sea shell powder with other reported low-cost adsorbents.

Sorbent	$q_{max}$ (mg g <sup>-1</sup> )	Reference
<i>Arundo donax</i> root carbon	8.69	[46]
Activated charcoal	0.179	[48]
Waste apricot	116.27	[49]
Activated carbons commercial grade	8.27	[50]
Laboratory grade activated carbons	42.18	[50]
Bentonite	7.72	[51]
Sugarcane dust	4.88	[52]
Degreased coffee bean	55.3	[39]
Hen feathers	26.1	[53]
Iron humate	19.2	[54]
Rubber wood sawdust	36.45	[55]
Cellulose	2.422	[56]
Treated sawdust	65.8	[41]
Neem leaf powder	133.6	[57]
<i>Ricinus communis</i>	27.78	[58]
Lemon peel	51.73	[59]
<i>Caulerpa racemosa</i> var. <i>cylindracea</i>	26.57	[60]
Rattan sawdust	62.7	[61]
Maize cob powder	37.037	[62]
Sea shell powder	42.33	Present study



powder are some of the additional advantages, reflecting a promising future for sea shell powder utilization in BG 4 removal from aqueous solutions.

## 5. Conclusion

In this study, the ability of sea shell powder to remove BG 4 from aqueous solution was investigated. The operational parameters such as pH, initial dye concentration, adsorbent dose, contact time, and temperature, were found to have an effect on the adsorption efficiency of sea shell powder. The maximum adsorption of BG 4 was found at pH 8. Maximum adsorption capacity was  $42.33 \text{ mg g}^{-1}$  at  $50 \text{ mg L}^{-1}$  initial BG 4 concentration. The temperature has strong influence on the adsorption process and the maximum removal was observed at 303 K. The equilibrium was attained at 120 min. Afterwards, there was no significant increase in BG 4 adsorption. Further, the adsorbent was characterized by Fourier Transform Infrared Spectroscopy (FTIR) and Scanning Electron Microscopy (SEM) techniques. The kinetic studies revealed that the adsorption process best fit the pseudo-second-order kinetic model. Intraparticle diffusion was not the sole rate-controlling step. The study on equilibrium sorption revealed that Langmuir isotherm model gave the best fit to experimental data. The nature of adsorption of BG 4 on sea shell powder was physical adsorption as inferred from the Dubinin–Radushkevich (D–R) isotherm model. The calculated thermodynamic parameters showed the exothermic and spontaneous nature of the adsorption of BG 4 onto sea shell powder. The present study showed that sea shell powder could be used as a good and inexpensive adsorbent for dye effluent treatment.

## Appendix A. Supplementary data

Supplementary data associated with this article can be found, in the online version, at doi:10.1016/j.cej.2010.08.050.

## References

- [1] V.K. Gupta, Suhas, Application of low-cost adsorbents for dye removal – a review, *J. Environ. Manage.* 90 (2009) 2313–2342.
- [2] P. Saha, Assessment on the removal of methylene blue dye using tamarind fruit shell as biosorbent, *Water Air Soil Pollut.*, 2010. doi:10.1007/s11270-010-r0384-2.
- [3] A. Demirbas, Agricultural based activated carbons for the removal of dyes from aqueous solutions: a review, *J. Hazard. Mater.* 167 (2009) 1–9.
- [4] V.K. Garg, R. Kumar, R. Gupta, Removal of Malachite Green dye from aqueous solution by adsorption using agroindustries waste: a case study of *Phosopis cineraria*, *Dyes Pigments* 62 (2004) 1–10.
- [5] A. Hashem, R.A. Akasha, A. Ghith, D.A. Hussein, Adsorbent based on agricultural wastes for heavy metal and dye removal: a review, *Energy Educ. Sci. Technol.* 19 (2007) 69–86.
- [6] S. Chowdhury, R. Mishra, P. Saha, Adsorption thermodynamics, kinetics and isosteric heat of adsorption of Malachite Green onto chemically modified rice husk, *Desalination*, 2010. doi:10.1016/j.desal.2010.07.047.
- [7] G. Crini, H.N. Peindy, F. Gimbert, C. Robert, Removal of C.I. Basic Green 4 (Malachite Green) from aqueous solution by adsorption using cyclodextrin-based adsorbent: kinetic and equilibrium studies, *Sep. Purif. Technol.* 53 (2007) 97–110.
- [8] P. Saha, S. Chowdhury, S. Gupta, I. Kumar, R. Kumar, Assessment on the removal of Malachite Green using tamarind fruit shell as biosorbent, *Clean: Soil Air Water* 38 (5–6) (2010) 437–445.
- [9] A. Srivastava, R. Sinha, D. Roy, Toxicological effects of Malachite Green, *Aquat. Toxicol.* 66 (2004) 319–329.
- [10] M. Rafatullah, O. Sulaiman, R. Hashim, A. Ahmad, Adsorption of methylene blue on low-cost adsorbents: a review, *J. Hazard. Mater.* 177 (2010) 70–80.
- [11] Z. Hu, H. Chen, F. Ji, S. Yuan, Removal of congo red from aqueous solution by cattail root, *J. Hazard. Mater.* 173 (2010) 292–297.
- [12] R. Narayanan, S. Dutta, S.K. Seshadri, Hydroxy apatite coatings on Ti–6Al–4V from seashell, *Surf. Coat. Technol.* 200 (2006) 4720–4730.
- [13] I. Langmuir, The constitution and fundamental properties of solids and liquids, *J. Am. Chem. Soc.* 38 (11) (1916) 2221–2295.
- [14] V.S. Mungapati, V. Yarramuthi, S.K. Nadavala, S.R. Alla, K. Abburi, Biosorption of Cu(II), Cd(II) and Pb(II) by *Acacia leucocephala* bark powder: kinetics, equilibrium and thermodynamics, *Chem. Eng. J.* 157 (2010) 357–365.
- [15] H.M.F. Freundlich, Over the adsorption in solution, *J. Phys. Chem.* 57A (1906) 385–470.
- [16] R. Nadeem, M.H. Nasir, M.S. Hanif, Pb(II) sorption by acidically modified *Cicer arietinum* biomass, *Chem. Eng. J.* 150 (2009) 40–48.
- [17] M.M. Dubinin, L.V. Radushkevich, The equation of the characteristic curve of the activated charcoal, *Proc. Acad. Sci. USSR Phys. Chem. Sect.* 55 (1947) 331–337.
- [18] M.M. Dubinin, The potential theory of adsorption of gases and vapours for adsorbents with energetically non-uniform surfaces, *Chem. Rev.* 60 (1960) 235–266.
- [19] S. Kundu, A.K. Gupta, Arsenic adsorption onto iron oxide-coated cement (IOCC): regression analysis of equilibrium data with several isotherm models and their optimization, *Chem. Eng. J.* 122 (2006) 93–106.
- [20] S. Lagergren, About the theory of so-called adsorption of soluble substances, *K. Sven. Vetenskapsakad. Handl* 24 (1898) 1–39.
- [21] Y.S. Ho, Citation review of Lagergren kinetic rate equation on adsorption reactions, *Scientometrics* 59 (2004) 171–177.
- [22] A. Gundogdu, D. Ozdes, C. Duran, V.N. Bulut, M. Soyulak, H.B. Senturk, Biosorption of Pb(II) ions from aqueous solution by pine bark (*Pinus brutia* Ten.), *Chem. Eng. J.* 153 (2009) 62–69.
- [23] Y.S. Ho, G. McKay, The sorption of lead (II) ions on peat, *Water Res.* 33 (1999) 578–584.
- [24] Y.S. Ho, G. McKay, Pseudo-second order model for sorption processes, *Process Biochem.* 34 (1999) 451–465.
- [25] S.G. Susmita, G.K. Bhattacharya, Adsorption of Ni (II) on clays, *J. Colloid Interface Sci.* 295 (2006) 21–32.
- [26] W.J. Weber, J.C. Morris, Kinetics of adsorption on carbon from solution, *J. Sanit. Eng. Div. Am. Soc. Civ. Eng.* 89 (1963) 31–60.
- [27] Z.-Y. Yao, J.-H. Qi, L.-H. Wang, Equilibrium, kinetic and thermodynamic studies on the biosorption of Cu(II) onto chestnut shell, *J. Hazard. Mater.* 174 (2010) 137–143.
- [28] M.V. Subbaiah, Y. Vijaya, N.S. Kumar, A.S. Reddy, A. Krishnaiah, Biosorption of nickel from aqueous solutions by *Acacia leucocephala* bark, *Colloids Surf. B* 74 (2009) 260–265.
- [29] J. Gao, Q. Zhang, R. Chen, Y. Peng, Biosorption of acid yellow 17 from aqueous solution by non-living aerobic granular sludge, *J. Hazard. Mater.* 174 (2010) 215–225.
- [30] S.M. de Oliveira Brito, H.M.C. Andrade, L.F. Soares, R.P. de Azevedo, Brazil nut shells as a new biosorbent to remove methylene blue and indigo carmine from aqueous solutions, *J. Hazard. Mater.* 174 (2010) 84–92.
- [31] A. Ahalya, R.D. Kanamadi, T.V. Ramachandra, Biosorption of chromium (VI) from aqueous solutions by the husk of Bengal gram (*Cicer arietinum*), *Electron. J. Biotechnol.* 8 (2005) 258–264.
- [32] P.X. Sheng, Y.P. Ting, J.P. Chen, L. Hong, Sorption of lead, copper, cadmium, zinc, and nickel by marine algal biomass: characterization of biosorptive capacity and investigation of mechanisms, *J. Colloid Interface Sci.* 275 (2004) 131–141.
- [33] M.A. Al-Ghouthi, J. Li, Y. Salamh, N. Al-Laqtah, G. Walker, M.N.M. Ahmad, Adsorption mechanisms of removing heavy metals and dyes from aqueous solution using date pits solid adsorbent, *J. Hazard. Mater.* 176 (2010) 510–520.
- [34] K. Vijayaraghavan, K. Palanivelu, M. Velan, Biosorption of copper(II) and cobalt(II) from aqueous solutions by crab shell particles, *Bioresour. Technol.* 97 (2006) 1411–1419.
- [35] N. Nasuha, B.H. Hameed, T. Azam, Mohd Din, Rejected tea as a potential low-cost adsorbent for the removal of methylene blue, *J. Hazard. Mater.* 175 (2010) 126–132.
- [36] S.T. Akar, A.S. Özcan, T. Akar, A. Özcan, Z. Kaynak, Biosorption of a reactive textile dye from aqueous solutions utilizing an agro-waste, *Desalination* 249 (2009) 757–761.
- [37] V.K. Garg, R. Kumar, R. Gupta, Removal of Malachite Green dye from aqueous solution by adsorption using agro-industry waste: a case study of *Prosopis cineraria*, *Dyes Pigments* 62 (2004) 1–10.
- [38] W.-T. Tsai, H.-R. Chen, Removal of Malachite Green from aqueous solution using low-cost chlorella-based biomass, *J. Hazard. Mater.* 175 (2010) 844–849.
- [39] M.-H. Baek, C.O. Ijagbemi, O. Se-Jin, D.-S. Kim, Removal of Malachite Green from aqueous solution using degreased coffee bean, *J. Hazard. Mater.* 176 (2010) 820–828.
- [40] S.D. Khattri, M.K. Singh, Removal of Malachite Green from dye wastewater using neem sawdust by adsorption, *J. Hazard. Mater.* 167 (2009) 1089–1094.
- [41] V.K. Garg, R. Gupta, A.B. Yadav, R. Kumar, Dye removal from aqueous solution by adsorption on treated sawdust, *Bioresour. Technol.* 89 (2003) 121–124.
- [42] Z. Aksu, Biosorption of reactive dyes by dried activated sludge: equilibrium and kinetic modeling, *Biochem. Eng. J.* 7 (2001) 79–84.
- [43] K. Kadirvelu, C. Karthika, N. Vennilamani, S. Pattabhi, Activated carbon from industrial solid waste as an adsorbent for the removal of rhodamine-B from aqueous solution: kinetic and equilibrium studies, *Chemosphere* 60 (2005) 1009–1017.
- [44] M. Ozacar, A.I. Sengil, Adsorption of metal complex dyes from aqueous solutions by pine sawdust, *Bioresour. Technol.* 96 (2005) 791–795.
- [45] G. Crini, P.M. Badot, Application of chitosan, a natural aminopolysaccharide for dye removal from aqueous solutions by adsorption processes using batch studies: a review of recent literature, *Prog. Polym. Sci.* 33 (2008) 399–447.
- [46] J. Zhang, Y. Li, C. Zhang, Y. Jing, Adsorption of Malachite Green from aqueous solution onto carbon prepared from *Arundo donax* root, *J. Hazard. Mater.* 150 (2008) 774–782.
- [47] T.S. Anirudhan, P.G. Radhakrishnan, Thermodynamics and kinetics of adsorption of Cu (II) from aqueous solution onto a new cation exchanger derived from tamarind fruit shell, *J. Chem. Thermodyn.* 40 (2008) 702–709.

- [48] M.J. Iqbal, M.N. Ashiq, Adsorption of dyes from aqueous solutions on activated charcoal, *J. Hazard. Mater.* B139 (2007) 57–66.
- [49] C.A. Basar, Applicability of the various adsorption models of three dyes adsorption onto activated carbon prepared apricot, *J. Hazard. Mater.* B135 (2006) 232–241.
- [50] I.D. Mall, V.C. Srivastava, N.K. Agarwal, I.M. Mishra, Adsorptive removal of Malachite Green dye from aqueous solution by bagasse fly ash and activated carbon-kinetic study and equilibrium isotherm analyses, *Colloids Surf. A* 264 (2005) 17–28.
- [51] S.S. Tahir, N. Rauf, Removal of a cationic dye from aqueous solutions by adsorption onto bentonite clay, *Chemosphere* 63 (2006) 1842–1848.
- [52] S.D. Khattri, M.K. Singh, Colour removal from dye wastewater using sugar cane dust as an adsorbent, *Adsorpt. Sci. Technol.* 17 (1999) 269–282.
- [53] A. Mittal, Adsorption kinetics of removal of a toxic dye, Malachite Green, from wastewater by using hen feathers, *J. Hazard. Mater.* B133 (2006) 196–202.
- [54] P. Janos, Sorption of basic dyes onto iron humate, *Environ. Sci. Technol.* 37 (2003) 5792–5798.
- [55] K.V. Kumar, S. Sivanesan, Isotherms for Malachite Green onto rubber wood (*Hevea brasiliensis*) sawdust: comparison of linear and non-linear methods, *Dyes Pigments* 72 (2007) 124–129.
- [56] C.P. Sekhar, S. Kalidhasan, V. Rajesh, N. Rajesh, Bio-polymer adsorbent for the removal of Malachite Green from aqueous solution, *Chemosphere* 77 (2009) 842–847.
- [57] K.G. Bhattacharyya, A. Sarma, Adsorption characteristics of the dye, brilliant green, on neem leaf powder, *Dyes Pigments* 57 (2003) 211–222.
- [58] T. Santhi, S. Manonmani, T. Smitha, Removal of Malachite Green from aqueous solution by activated carbon prepared from the epicarp of *Ricinus communis* by adsorption, *J. Hazard. Mater.* 179 (2010) 178–186.
- [59] K.V. Kumar, Optimum sorption isotherm by linear and non-linear methods for Malachite Green onto lemon peel, *Dyes Pigments* 74 (2007) 595–597.
- [60] Z. Bekci, Y. Seki, L. Cavas, Removal of Malachite Green by using an invasive marine alga *Caulerpa racemosa* var. *cylindracea*, *J. Hazard. Mater.* 161 (2009) 1454–1460.
- [61] B.H. Hameed, M.I. El-Khaiary, Malachite Green adsorption by rattan sawdust: isotherm, kinetic and mechanism modeling, *J. Hazard. Mater.* 159 (2008) 574–579.
- [62] G.H. Sonawane, V.S. Shrivastava, Kinetics of decolourization of Malachite Green from aqueous medium by maize cob (*Zea mays*): an agricultural solid waste, *Desalination* 247 (2009) 430–441.